






Genetic changes and growth promotion of glioblastoma by magnetic nanoparticles and a magnetic field

Seung-Hyun Yang^{1,2} , Byunghoon Kang³, Yuna Choi², Hyun Wook Rho², Hye Young

Son^{‡,*,2,4}  & Yong-Min Huh^{‡,**,2,4,5,6} 

¹Interdisciplinary Program in Nanomedical Science & Technology, Nanomedical National Core Research Center, Yonsei University, Seoul, 03722, Republic of Korea

²Department of Radiology, College of Medicine, Yonsei University, Seoul, 03722, Republic of Korea

³BioNanotechnology Research Center, Korea Research Institute of Bioscience & Biotechnology (KRIBB), Daejeon, 34141, Republic of Korea

⁴Severance Biomedical Science Institute, College of Medicine, Yonsei University, Seoul, 03722, Republic of Korea

⁵Department of Biochemistry & Molecular Biology, College of Medicine, Yonsei University, Seoul, 03722, Republic of Korea

⁶YUHS-KRIBB Medical Convergence Research Institute, College of Medicine, Yonsei University, Seoul, 03722, Republic of Korea

*Author for correspondence: Tel.: +82 2 2228 0886; shy916@yuhs.ac

**Author for correspondence: Tel.: +82 2 2228 0874; ymhuh@yuhs.ac

‡Authors contributed equally

Aim: To confirm the biological effects of manganese ferrite magnetic nanoparticles (MFMNPs) and an external magnetic field on glioblastoma cells. **Methods:** U-87MG glioblastoma cells were prepared, into which the uptake of MFMNPs was high. The cells were then exposed to an external magnetic field using a neodymium magnet *in vitro* and *in vivo*. **Results:** *LRP6* and *TCF7* mRNA levels involved in the Wnt/ β -catenin signaling pathway were elevated by the influence of MFMNPs and the external magnetic field. MFMNPs and the external magnetic field also accelerated tumor growth by approximately 7 days and decreased survival rates in animal experiments. **Conclusion:** When MFMNPs and an external magnetic field are applied for a long time on glioblastoma cells, mRNA expression related to Wnt/ β -catenin signaling is increased and tumor growth is promoted.

First draft submitted: 12 October 2020; Accepted for publication: 19 March 2021; Published online: 23 April 2021

Keywords: external magnetic field • glioblastoma • manganese ferrite magnetic nanoparticles • tumor growth • Wnt/ β -catenin signaling

Magnetic nanoparticles (MNPs) have mostly been studied as MRI contrast agents, drugs and gene carriers. MNPs have also been researched and developed in various fields involving the application of their magnetic characteristics, particularly artificial receptor clusterization for cell growth signaling, cell capture using microfluidic chips, and *in vivo* control of stem cell migration and differentiation [1–3]. As the number of studies using MNPs and magnetic fields has increased, studies on the correlation between MNPs and magnetic fields have been conducted. In MNPs, raw materials, sizes and surface charges are related to cytotoxicity, and there are many opinions on the genetic changes they can cause [4,5].

A high-strength static magnetic field (4.7 T) alters the ability of human malignant melanoma cells to remain adherent to their tissue culture surface but does not have the same effect on normal human fibroblasts [6]. In addition, a stronger static magnetic field (7 T) delays the growth of three human tumor cell lines [7]. Recent studies have shown that a magnetic field can cause physical interactions that can change mesenchymal stem cell shape, function and fate [8]. For example, a static magnetic field produced MNP aggregates that induced an unsuspected cytotoxicity effect both *in vitro* and *in vivo* [9]. In addition, MNPs might induce apoptosis by an extremely low-frequency magnetic field [10]. Nevertheless, many studies using MNPs and magnetic field have been conducted. For example, anti-Frizzled functionalized MNPs and magnets activated the Wnt/ β -catenin signaling pathway in

human mesenchymal stem cells [11]. In one study of hyperthermia treatment, an external alternating magnetic field killed cancer cells by the effect of raising the temperature around the MNPs [12]. Despite the high biological and medical application potential of MNPs, studies on MNPs and magnetic field interaction have not been conducted sufficiently. The opinions on its influence also vary [13–16].

Manganese ferrite MNPs (MFMNPs) have been demonstrated not only to have higher magnetization than other metal-doped iron oxide nanoparticles, such as CoFe_2O_4 and NiFe_2O_4 , but also to enable ultrasensitive targeted MRI *in vivo*. MFMNPs have previously shown great potential as T2 contrast agents because they greatly improve cancer cell detection sensitivity and enable *in vivo* MRI of small tumors [17]. In addition, MFMNPs can be phase-transferred using amphiphilic polymers and functionalized, making it easy to attach antibodies, peptides or other molecules to them. For these reasons, MFMNPs have been primarily studied as agents for molecular MRI, multimodal imaging, drug delivery and gene delivery [18–21].

This study utilized MFMNPs and an external magnetic field to assess the changes they elicited in tumor cell mRNA expression levels and tumor growth. To ensure high uptake of MFMNPs into U-87MG glioblastoma cells, the well-known transfection agent poly-L-lysine (PLL) was used. Cells containing MFMNPs were then exposed to an external magnetic field using a neodymium magnet. Following this, the level of Wnt/ β -catenin signaling-related mRNA expression *in vitro* was confirmed. Tumor growth, metastasis and survival were also confirmed in animal models.

Materials & methods

Materials

1,2-hexadecanediol, manganese(II) acetylacetonate, iron(III) acetylacetonate, dodecanoic acid, dodecylamine, benzyl ether and polysorbate 80 were purchased from Sigma-Aldrich (MO, USA). Phosphate-buffered saline (PBS, 10mM, pH 7.4), Dulbecco's modified Eagle medium, fetal bovine serum and antibiotic–antimycotic solution were purchased from Thermo Fisher Scientific (Gibco, MA, USA). U-87MG cells were purchased from the American Type Culture Collection (VA, USA). The CCK-8 assay kit was purchased from Dojindo Molecular Technologies, Inc. (MD, USA). Ultrapure deionized water was used for all syntheses. All other chemicals and reagents were analytical grade.

Synthesis of MFMNPs

The thermal decomposition method was used to synthesize monodispersed MFMNPs [22]. The method was performed according to previously reported procedures [17]. Iron(III) acetylacetonate (2 mmol), manganese(II) acetylacetonate (1 mmol), 1,2-hexadecanediol (10 mmol), dodecanoic acid (6 mmol) and dodecylamine (6 mmol) were dissolved in 20 ml benzyl ether under nitrogen gas atmosphere [23]. The mixture was then preheated at 200°C for 2 h and refluxed at 300°C for 30 min. After reflux, the reactants were cooled at room temperature sufficiently and then purified with an excess of 99.9% ethanol. MFMNPs were synthesized up to approximately 12 nm in diameter using the seed-mediated growth method. MFMNP seeds (100 mg) were dispersed in 4 ml hexane, then the mixture was heated to a maximum of 100°C at 10°C/min, stirred for 30 min to remove hexane, then heated again at 200°C. These processes were performed twice to get 12-nm MFMNPs.

Preparation of MFMNPs

MFMNPs were prepared by the nanoemulsion method [19]. MFMNPs were dissolved in hexane (7.5 mg/ml, organic phase). The amphiphilic polymer polysorbate 80 was dissolved in deionized water (5 mg/ml, aqueous phase). The two solutions were mixed and sonicated using a Teflon impeller in a 4°C bath for 15 min. The remaining hexane was evaporated overnight at room temperature, and the products were concentrated and purified using a centrifugal filter (Centriprep YM-3, Merck, Darmstadt, Germany). The hydrodynamic size distribution of MFMNPs was analyzed by dynamic laser scattering (ELS-Z, Otsuka Electronics Co., Osaka, Japan). The morphology of MFMNPs was confirmed using transmission electron microscopy (JEM-2100, JEOL, Tokyo, Japan). The Mn and Fe ion concentrations from nanoparticles were calculated by inductively coupled plasma–optical emission spectrometer.

Cytotoxicity

To evaluate the cytotoxicity of MFMNPs, the CCK-8 cell proliferation/cytotoxicity assay kit was used. U-87MG cells were seeded into a 96-well culture plate (2×10^4 cells/well) and cultured for 24 h at 37°C in a humidified atmosphere with 5% CO_2 . Cells were treated with MFMNPs and MFMNPs with PLL at various concentrations

for 24 h. For the MFMNPs with PLL, 25 $\mu\text{g}/\text{ml}$ MFMNPs were incubated with PLL (1.5 $\mu\text{g}/\text{ml}$) for 5 min, serially diluted twofold to make nine aliquots and administered to U-87MG cells for 24 h. After treatment, cells were treated with the CCK-8 solution according to the manufacturer's instructions. Cell viability was evaluated spectrophotometrically using a microplate reader (Synergy H1, BioTeck Instruments, VT, USA) at 450 nm. All experiments were performed in triplicate. The PLL concentration was determined according to the method reported by Yun *et al.* [1].

Prussian blue staining

Prussian blue staining was used to evaluate the efficacy of the delivery of MFMNPs using PLL. Based on the results of cytotoxicity experiments, the concentrations of MFMNPs (25 $\mu\text{g}/\text{ml}$) and PLL (1.5 $\mu\text{g}/\text{ml}$) were determined. First, U-87MG cells (2×10^6) were incubated with MFMNPs for 4 h at 37°C . Second, the cells were washed with warm PBS and then fixed with 4% paraformaldehyde. Third, to dye the MNPs, 10% potassium ferrocyanide and 20% hydrochloric acid were mixed in a 1:1 ratio. The fixed U-87MG cells were treated with the mixed dye solution for 30 min at room temperature. After staining, the cells were washed with deionized water, and the nucleus was counterstained for 30 min using a nuclear fast red solution (Sigma-Aldrich, MO, USA). Finally, the cells were observed using an optical microscope (CKX41, Olympus, Tokyo, Japan).

Migration assay

To evaluate the migration effects under an external magnetic field, 25 $\mu\text{g}/\text{ml}$ MFMNPs were incubated with 1.5 $\mu\text{g}/\text{ml}$ PLL for 5 min and added to a trypsinized single-cell suspension of U-87MG cells (2×10^6). After 4 h, cells were washed with PBS thrice, seeded in six-well plates (2.5×10^5 cells/well) and cultured at 37°C in a humidified atmosphere with 5% CO_2 . After 1 day, the half-side of the wells was wiped out with a cell scraper, and the neodymium magnets were attached on the right side of the wells. Cells were observed daily using an optical microscope.

Quantitative real-time PCR

Whole RNA was purified using MasterPure™ RNA purification kit (Epicentre Biotechnologies, WI, USA) according to the manufacturer's protocol. The RNA concentration was determined using the Nanodrop 2000 spectrophotometer (Thermo Fisher Scientific, MA, USA). cDNA was synthesized from 1000 ng total RNA using a High-Capacity RNA-to-cDNA kit (Applied Biosystems, CA, USA). qRT-PCR was performed using a SensiFAST™ SYBR® Lo-ROX kit (Bioline, Luckenwalde, Germany), and PCR was executed using a ViiA 7 Real-time PCR System (Thermo Fisher Scientific, MA, USA). PCR was performed in triplicate, and samples were normalized to *GAPDH* and β -actin expression levels. The PCR was performed 40 cycles as follows: 3 min initial denaturation at 95°C , denaturation at 95°C for 10 s each, annealing at 60°C for 30 s each, extension at 72°C for 30 s and then 72°C for 5 min for a final extension.

Mouse tumor modeling

Male athymic BALB/c nude mice aged 5 weeks (Orient Bio, Seongnam, Korea) were used for tumor xenograft experiments. Mice were retained in microisolator cages under sterile conditions and observed for at least 1 week before the study initiation to ensure proper health. Temperature, lighting and humidity were controlled centrally. All experimental procedures were approved by the Yonsei University College of Medicine Institutional Animal Care and Use Committee and were carried out in accordance with the committee's guidelines. Before the experiments, all mice were anesthetized with 2% isoflurane. In the heterotopic xenograft mouse model, 2×10^6 U-87MG cells were implanted into the right thigh using a 29-gauge needle. The orthotopic brain tumor xenograft model was drilled on the mouse skull using a 26-gauge needle. U-87MG cells (1×10^5) were implanted directly into the right frontal lobe of nude mice using a Gastight syringe (Hamilton Co., NV, USA) at a depth of 4.5 mm. Cells were simultaneously injected into each mouse using a multiple microinfusion syringe pump (Harvard Apparatus, MA, USA) at a rate of 0.5 $\mu\text{l}/\text{min}$, as described previously [24]. After U-87MG implantation, ring-type 3000-gauge neodymium magnets were attached to the right thigh, and 2000-gauge disk-type neodymium magnets were attached to the forehead using a medical adhesive (3M Vetbond Tissue Adhesive, 3M Co., MN, USA). While transplanting U-87MG glioblastoma cells, tumor growth could generally be visually confirmed from about 3 weeks. Because the MFMNPs were able to maintain their magnetic properties for 2 or more weeks even after entering the mouse's body, neodymium magnets were attached for 2 weeks (Supplementary Figure 1). Each mouse was housed

in a separate cage to avoid the influence of magnets attached to other mice. The tumor volume and survivals were recorded at least twice a week (tumor volume was measured after the removal of the magnets).

Magnetic resonance imaging

T2-weighted MRI experiments were investigated with a 9.4 T Bruker 20-cm bore animal MRI system (Biospec 94/20 USR, Bruker Medical Systems, Karlsruhe, Germany) equipped with a 40-mm inner diameter quadrature radiofrequency coil (RF SUC 400 1H M-BR-LIN Road, Bruker Medical Systems, Karlsruhe, Germany). For animal MRI, anesthesia was induced by 3% and maintained with 2% isoflurane in a mixture of 70% N₂O and 30% O₂. The respiration rate was monitored with a small animal respiration pad (Model 1025 Small Animal Monitoring and Gating System; SA Instruments, Inc., NY, USA), and the body temperature was supported by a warm-water tube integrated into the animal bed. Magnetic resonance images were acquired with the following sequence: coronal T2-weighted rapid acquisition with relaxation enhancement (repetition time = 1800 ms, echo time = 22.2 ms, slice thickness = 0.50 mm, acquisition matrix = 274 × 200, field of view = 2.50 × 1.80 cm, flip angle = 180.0°). The relaxivity values of R2 were calculated by a series of T2 values when plotted as 1/T2 versus Fe and Mn. The relaxivity coefficient (mM⁻¹ s⁻¹) was equal to the ratio of R2 (1/T2; s⁻¹) to the MFMNP concentration.

Results

Characterization of MFMNPs

The morphology and size of MFMNPs were confirmed using transmission electron microscopy. In the electron microscope image, there was no abnormality in the appearance of MFMNPs and the size was constant and monodisperse. After nanoemulsion, the hydrodynamic size of MFMNPs was 36.2 ± 10.3 nm as determined by dynamic light scattering (Figure 1A). The potential magnetism to serve as an MRI contrast agent was confirmed using a 9.4-T animal MRI system. As the concentration of MFMNPs increased, the T2 relaxivities (R2) of MFMNPs linearly increased and the T2 relaxivity coefficient was 462.2 mM⁻¹ s⁻¹ (Figure 1B). The relaxivity reflected how the relaxation rates of MNPs changed as a function of concentration. The R2 value was defined as the ratio of Fe concentration that MFMNPs contained to the inverse of the T2 relaxation time, measured by the magnetic resonance signal intensity from the difference of T2 relaxation times. These results suggested that MFMNPs were stably dispersed in the aqueous phase, with the potential to be used as a T2 MR contrast agent, and that susceptibility could be sufficiently obtained by an external magnetic field in an experiment to be conducted in the next step.

Cytotoxicity & cellular affinity of MFMNPs with PLL

PLL is a cationic polymer used for gene transfection and MNP transfer to cells [2]. To determine the cytotoxicity of MFMNPs and PLL, the viability of U-87MG cells exposed to various concentrations of each condition was evaluated (Figure 2A). Cytotoxicity was assessed using the CCK-8 assay in ten concentrations. The highest concentrations were 25 µg/ml MFMNPs and 15 µg/ml PLL diluted twofold to make nine aliquots. There was no significant cytotoxicity until 25 µg/ml treated MFMNPs. In treated MFMNPs with PLL, only the 25 µg/ml condition showed about 85% cell viability. All subsequent experiments were conducted at MFMNP concentrations resulting in >85% cell viability. To evaluate higher cellular uptake efficiency using PLL, Prussian blue staining was carried out. Magnetic ions in cells treated with MFMNPs and MFMNPs with PLL were combined with injected ferrocyanide, resulting in the appearance of a bright blue color. In U-87MG cells treated with PLL and MFMNP, several blue spots could be observed by Prussian blue staining (Figure 2B). These results indicated that the cellular delivery of MFMNPs using PLL is safe and effective.

Migration effects of an external magnetic field

Cell migration experiments with an external magnetic field were performed for three reasons: to confirm the change in cell migration, to confirm the change in mRNA expression level produced by an external magnetic field and to check the magnetic field was of sufficient distance for the next animal experiment. To evaluate the migration effects of an external magnetic field, U-87MG cells were cultured in six-well culture plates under various conditions. Neodymium magnets were attached to the right side of the wells, and cells were observed daily using a microscope. On day 2, cells with MFMNPs and PLL under magnetic field were growing toward the magnets more than in the other conditions. On day 3, the difference in cell distribution was clearly confirmed. There were no significant differences in U-87MG cells using magnets, MFMNPs or PLL alone (Figure 3). In addition, the movement of

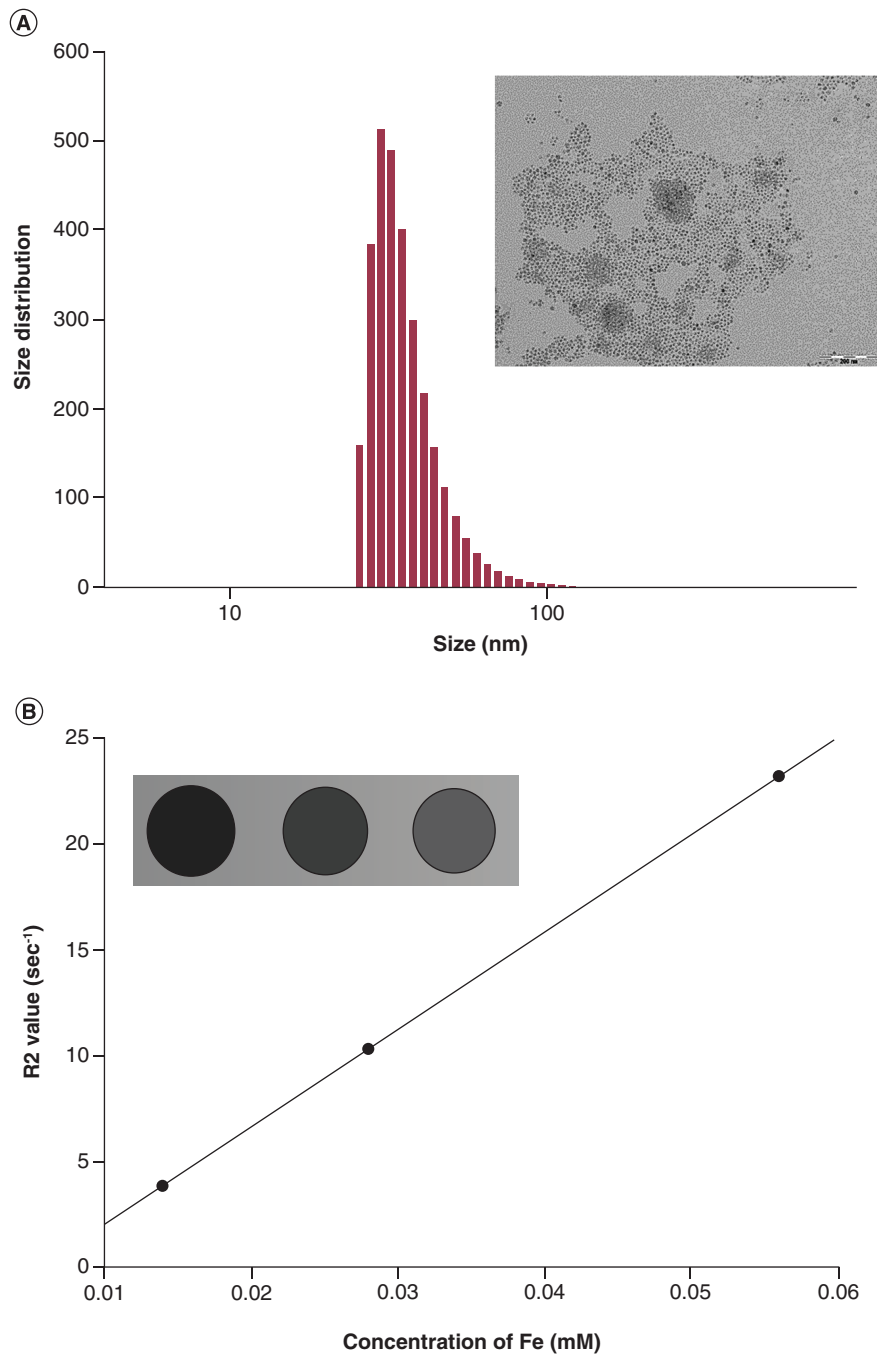


Figure 1. Characterization of manganese ferrite magnetic nanoparticles. (A) Hydrodynamic size and transmission electron microscopy image of manganese ferrite magnetic nanoparticles. **(B)** T2 MRI and graph for relaxivity coefficients around manganese ferrite magnetic nanoparticles.

cancer cells containing MFMNPs toward the magnet showed that the distance between the magnet and the cell was close enough to affect the cell. Because the diameter of one well of a six-well plate was 3.5 cm, the distance from the outermost surface of the cells to the magnet was predicted to be about 1.75 cm. Therefore the distance between cells and magnets was kept within 1.75 cm in the next *in vivo* experiment.

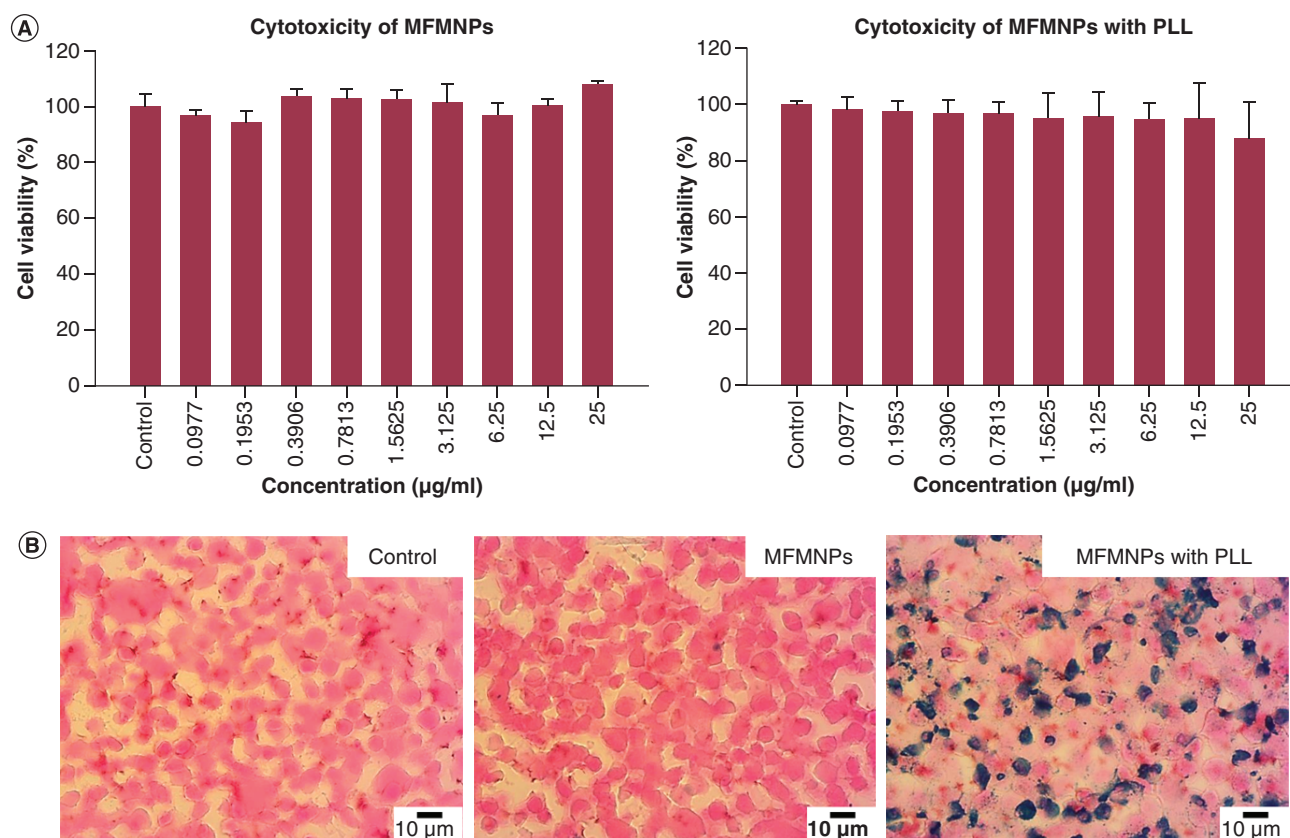


Figure 2. Cell viability and effects of poly-L-lysine. (A) CCK-8 assay of U-87MG glioblastoma cells using MFMNPs and MFMNPs with PLL. **(B)** Prussian blue staining of U-87MG glioblastoma cells. The ionic iron of MFMNPs reacts with acid ferrocyanide, producing a blue color. MFMNP: Manganese ferrite magnetic nanoparticle; PLL: Poly-L-lysine.

Confirmation of mRNA expression change by an external magnetic field

After the cell migration experiment, cells were trypsinized and RNA was purified. Then the expression levels of seven mRNAs – *Axin2*, *LRP6*, *TCF7*, *MYCN*, *SP5*, *ID2* and *EPHB3*, known to be increased due to chronic metabolic stress in cancer stem cell-like cells – were measured [25]. Under external magnetic field conditions, *LRP6* and *TCF7* mRNA levels were elevated, but changes in the levels of the other five mRNAs could not be confirmed as significant (Figure 4). In the qRT-PCR analysis, both mRNAs increased only when affected by MFMNPs, PLL and the external magnetic field, but did not increase significantly when only one or two of these three conditions were affected. The mRNA level was slightly increased in the magnet-only group, but this phenomenon was also observed for all other mRNAs. mRNA expression was normalized to the endogenous reference genes (*β-actin* and *GAPDH*) in the corresponding samples relative to untreated cells. These results demonstrated that MFMNP and an external magnetic field affect mRNA expression.

Effects of the external magnetic field on tumor growth & metastasis

To confirm the effects of MFMNPs and the external magnetic field in the *in vivo* model, U-87MG glioblastoma cells (treated with MFMNPs and untreated) were implanted in the right thigh of each of the three mice, and magnets were placed on the thighs for 2 weeks. All mice were isolated in separate cages to avoid the influence of other magnets. After removing the magnet, the tumor volume was recorded at least twice a week. Interestingly, when the tumors of each of the three mice grew measurably, the external magnetic field accelerated the tumor growth rate by 7 days (Figure 5A & B). It took 24 days for the tumor sizes of the three mice unaffected by the external magnet to be measurable, but only 17 days to measure the tumor size in mice affected by the external magnet. In addition, when U-87MG cells without MFMNPs were implanted and only magnets were attached, it

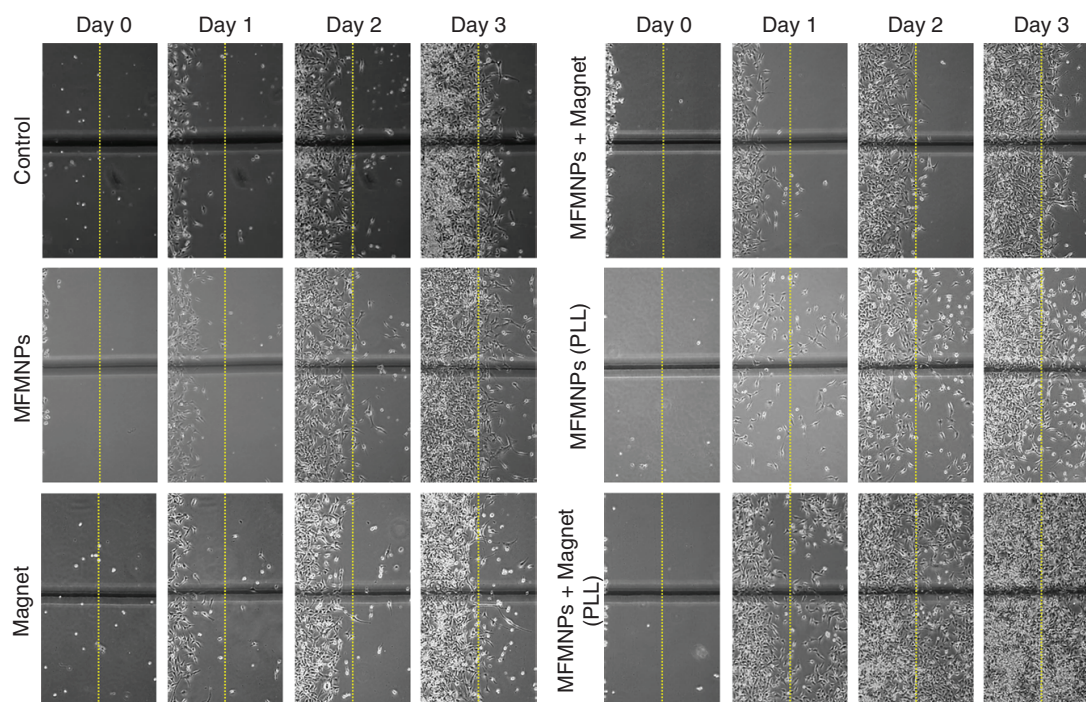


Figure 3. Cell migration assay with external magnetic field under various conditions. The magnets were located on the right side of each well.

MFMNP: Manganese ferrite magnetic nanoparticle; PLL: Poly-L-lysine.

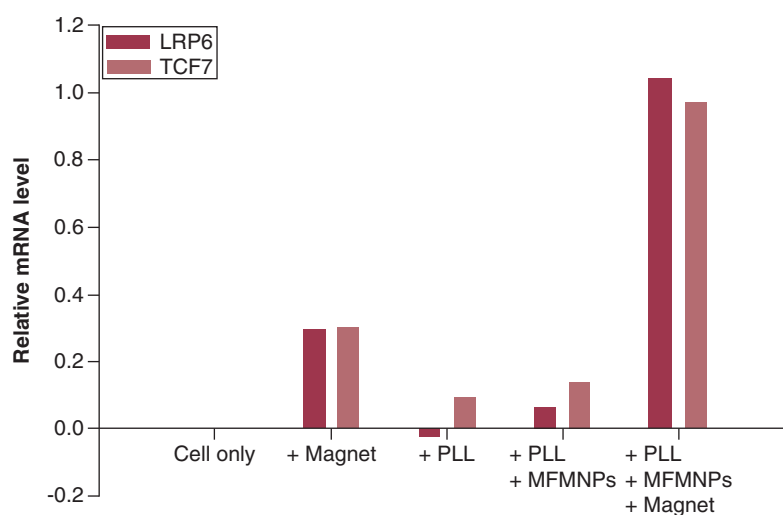


Figure 4. qRT-PCR graph of *LRP6* and *TCF7* mRNA under various conditions. U-87MG glioblastoma cells were exposed to an external magnetic field for 72 h.

MFMNP: Manganese ferrite magnetic nanoparticle; PLL: Poly-L-lysine.

took 22 days to measure the tumors in the three mice (Figure 5C). The tumor grew slightly faster; this result was predicted to be associated with the slight increase in the mRNA levels of *LRP6* and *TCF7* when cells were treated with magnets only in the *in vitro* qRT-PCR experiments (Figure 4). After 33 days, the animal experiment was ended according to the humane end point criteria, and the tumors were confirmed by MRI.

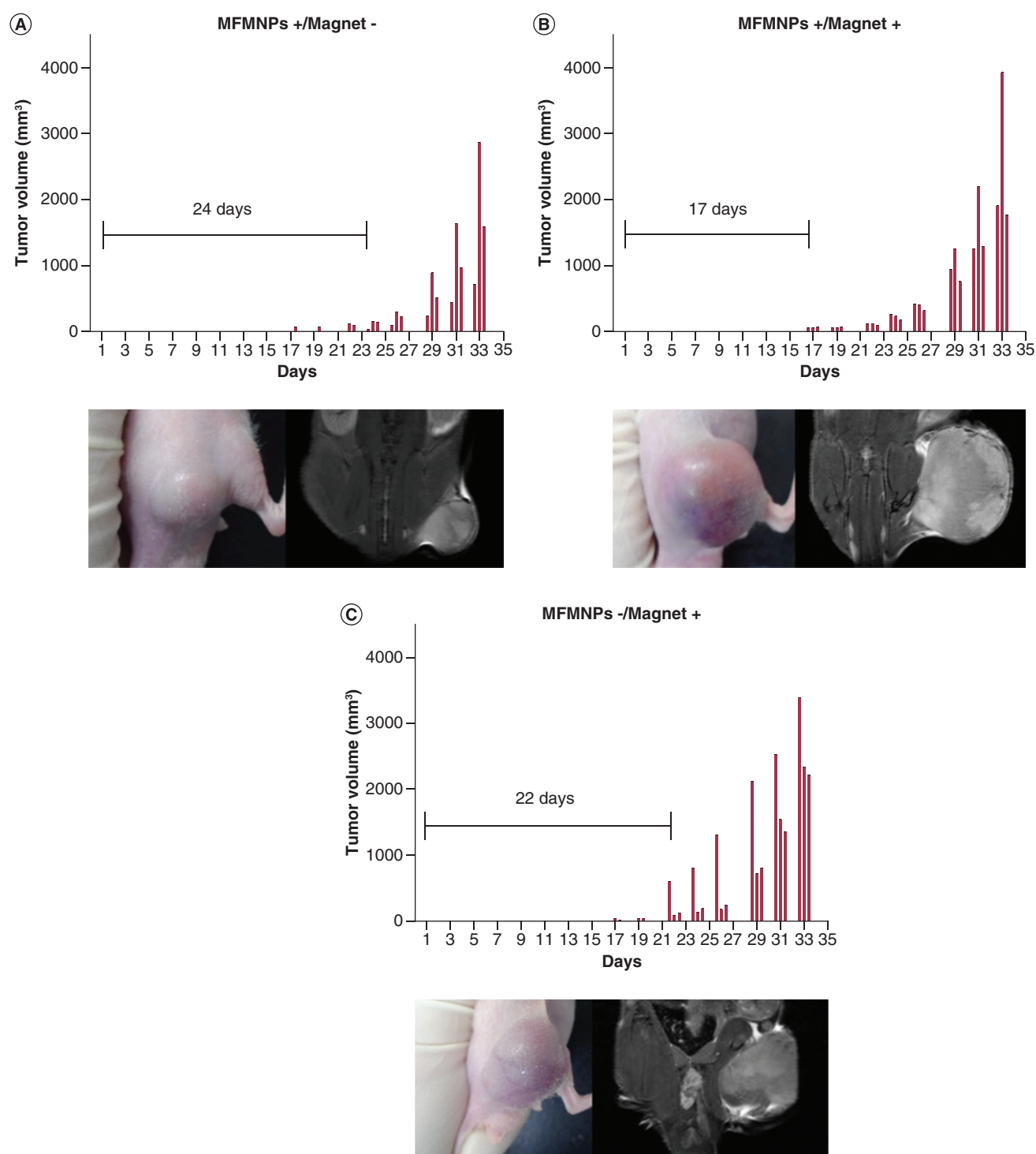


Figure 5. Increased tumor growth by manganese ferrite magnetic nanoparticles and external magnetic field. Graph of mouse tumor volume and the first day when tumor size could be measured in all three mice. The photos and magnetic resonance images were taken on day 33.

Magnet: External magnetic field; MFMNP: Manganese ferrite magnetic nanoparticle.

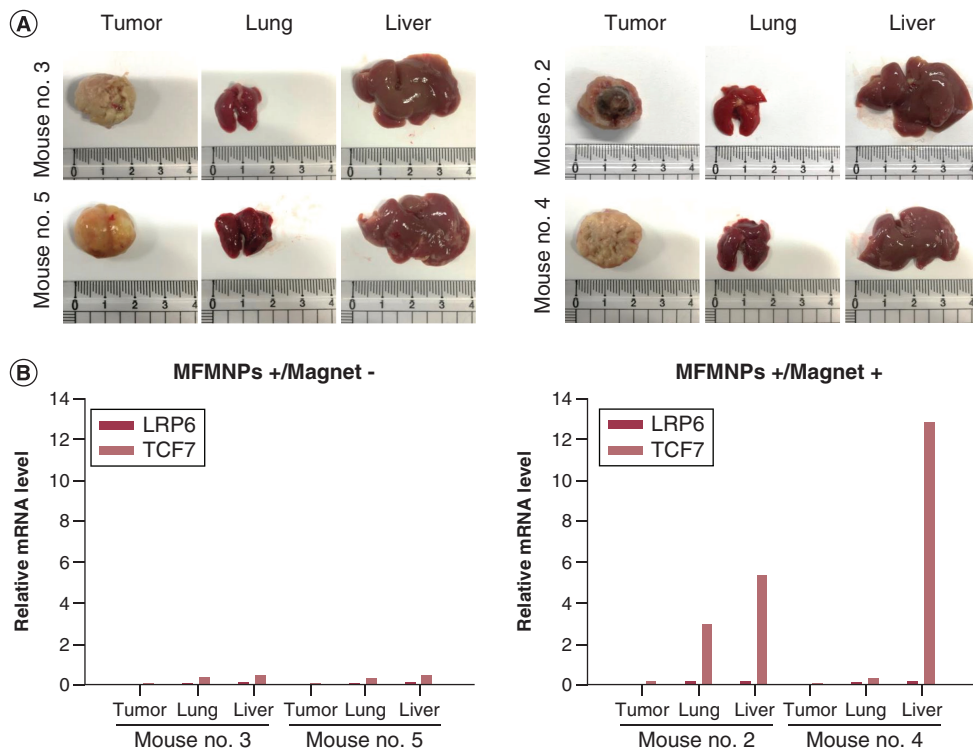


Figure 6. Effects of manganese ferrite magnetic nanoparticles and external magnetic field on tumor metastasis and mRNA expression. (A) Photographs of organs of each mouse. (B) *LRP6* and *TCF7* qRT-PCR graph of the tumors, lungs and liver.

Magnet: External magnetic field; MFMPN: Manganese ferrite magnetic nanoparticle.

After the tumor growth experiment, metastasis was confirmed for each mouse. In mice transplanted with U-87MG glioblastoma cells treated with only MFMPNs and those with U-87MG glioblastoma cells treated with MFMPNs and attached magnets, two of three mice in each group showed metastasis to the lungs and liver (Figure 6A). Interestingly, in the mouse group with only the magnet attached, metastasis could not be identified in the lungs or liver (Supplementary Figure 2).

LRP6 and *TCF7* mRNA expression levels were identified in primary tumors, lungs and liver. The number of metastatic tumor nodules was similar, but the level of mRNA expression was different. As shown in Figure 6B, the *LRP6* mRNA level showed no particular difference between the groups, but *TCF7* mRNA expression was higher in the liver and lung tissues of mice affected by external magnets than in mice not affected by external magnets.

These results provide evidence that changes in *TCF7* expression occur when both MFMPNs and external magnetic fields affect glioblastoma. Given that metastatic cancer can occur under various conditions, the influence of MFMPNs and external magnets does not unconditionally cause metastasis. The difference in the amount of *TCF7* expression may have occurred depending on the degree of metastatic cancer development (size and severity of the neoplasm).

Change of survival rate in the orthotopic xenograft model

U-87MG cells were implanted with MFMPNs in the right frontal lobe of ten mice, and the effect of the external magnetic field on survival was confirmed. Because space inside the skull is limited, it was predicted that if the rate of tumor growth were different between the groups, there would be differences in mouse survival. Tumor size was checked using MRI once a week. After 14 days, the tumor under the external magnet was bigger than in the other conditions (Figure 7A). After 23 days, only one mouse affected by an external magnet had survived, but five unaffected mice survived (Figure 7B). In the orthotopic xenograft model, the distance between the tumor cells and the magnet was slightly longer than in the heterotopic xenograft model; however, it was a sufficient distance to

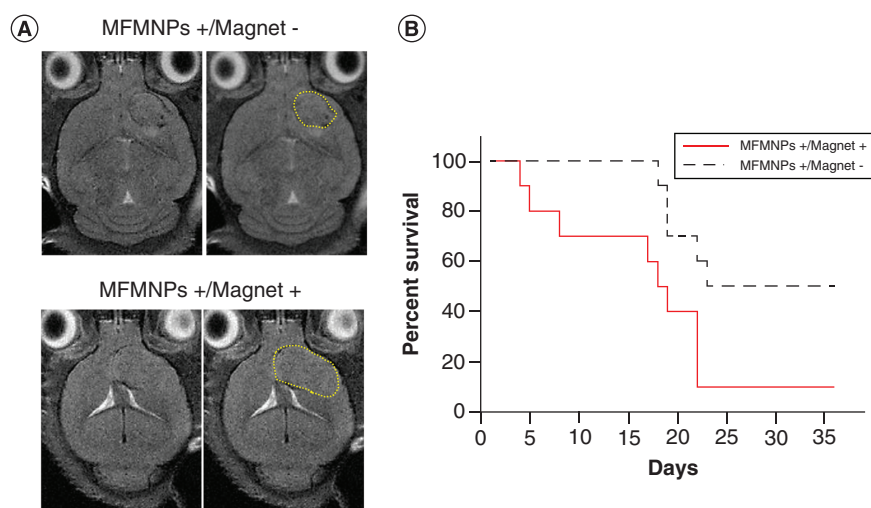


Figure 7. MRIs and survival graph of the orthotopic xenograft model. (A) T2 MRI of a mouse brain on day 14. Tumors are indicated by yellow dashed lines. **(B)** Kaplan–Meier survival graph of mice with and without an external magnetic field.

Magnet: External magnetic field; MFMNP: Manganese ferrite magnetic nanoparticle.

promote the growth of tumor cells. These results demonstrated that MFMNPs and the external magnetic field had an effect in both heterotopic and orthotopic xenograft models. Because the brain has limited internal space, the difference in the rate of tumor growth is more pronounced.

Discussion

Experimental data on the risks of nanoparticles published in the field of nanotoxicology have grown steadily in the past 20 years. The potential for problems arises from the inherent physicochemical properties (material, size, surface charge, etc.) of nanoparticles and their interaction with living organisms and complex biological environments. The magnetic field is known to have biological influences in some specific situations, such as high-strength static magnetic field [26]. However, most of these effects do not have fatal consequences [27]. Many MNPs have been used to target tumor cells using a magnetic field to improve efficacy in molecular imaging, drug delivery, gene delivery, cell isolation and therapeutic applications. However, little is known about what happens after cancer cells are constantly exposed to MNPs and an external magnetic field.

Therefore this study focused on the effects of MNPs and an external magnetic field on tumor cells. Placing a neodymium magnet near a glioblastoma cell treated with MNPs showed that cells grew toward the magnet over time and were affected by the external magnetic field. It was confirmed that the expression of two *Wnt*/ β -catenin signaling-related mRNAs was increased in glioblastoma cells affected by MNPs and the external magnetic field. Expression of these two mRNAs did not change significantly when only MNPs were used or when only the external magnetic field was used, but they increased significantly when both conditions were applied together.

LRP6 is a coreceptor with LRP5 and Frizzled protein family members which transmit signals by *Wnt* proteins through the canonical *Wnt*/ β -catenin signaling pathway. *Wnt* binding to *Fzd*/LRP6 activates what has traditionally been considered a linear signaling cascade, leading to the stabilization of β -catenin. Increased *LRP6* expression is known to trigger *Wnt* activation, cell proliferation and, typically, tumorigenesis [28–30]. In colorectal cancer, LRP6 promotes invasion and metastasis through cytoskeleton dynamics [31]. Hence LRP6 is recognized and studied as a promising anticancer target.

The *TCF7* protein binds to β -catenin and plays an essential role in *Wnt* signaling. After binding to β -catenin, the β -catenin/*TCF7* complex activates the transcription of the *Wnt* target gene and, as a result, promotes cell growth and cell migration [32]. *TCF7* was overexpressed in several malignant tumors, such as colorectal and breast tumors [33–35] and its expression is correlated with cellular proliferation, invasion or metastasis in gastric and lung cancers.

Because both mRNAs (*LRP6* and *TCF7*) are known to promote tumor growth, the tumor growth rate was confirmed by implanting glioblastoma cells containing MNPs into BALB/c nude mice. MFMNPs were introduced into glioblastoma cells using a cationic polymer, PLL, and then implanted into mice. If a magnetic field is used to introduce MFMNPs into glioblastoma cells, it is expected that the amount of nanoparticles introduced into cells will increase [36]. However, in Prussian blue-stained images, a sufficient number of particles were introduced into cells using only PLL. In addition, because this study refers to changes in mRNA expression when MFMNPs are introduced into cells and under the influence of an external magnetic field, the intervention of the external magnetic field should be minimized in the process of introducing MFMNPs. Also, because MFMNPs were introduced into glioblastoma cells and then transplanted into mice, it is unlikely that MFMNPs will have a toxic effect on normal cells or normal tissues. Because all MFMNPs were used at a cell viability concentration of 80% or more using the CCK-8 assay kit, the experimental results should be viewed as demonstrating the influence of MFMNPs and the external magnetic field rather than the toxicity of MFMNPs. In all animal experiments, there were no acute deaths or abnormal behaviors caused by the MFMNPs or external magnetic fields. After the end of the animal experiment, the organs of each mouse were checked, and there was no bleeding, swelling or inflammation other than metastatic cancer.

In a model with a heterotopic xenograft on the thigh of a mouse, glioblastoma cells affected by both the MFMNPs and external magnetic field grew 1 week faster than the control group. Liver and lung metastases were identified in each group. Interestingly, *TCF7* expression was very high in the liver tissues of mice, influenced by both the MFMNPs and external magnetic field, while the level of both mRNAs was low in the primary tumor. This is probably because the mRNA expression level changes as the tumor grows [37,38]. In a tumor metastasized to the lung or liver, it is expected that *TCF7* expression could be confirmed because it began to grow later than the primary cancer. *TCF7* is an important factor in metastasis, and overexpressed *TCF7* has been shown to be correlated with metastasis and low survival rate [39,40]. It is believed that these characteristics of *TCF7* also appeared in the mouse model in the study. Even when glioblastoma cells were transplanted into the mouse brain, the tumor growth of mice affected by MFMNPs and the external magnetic field was faster than in the control group; as a result, survival was poorer than in the control group.

Three mice died in the early days (4–7 days after tumor cell implantation) in an orthotopic xenograft model experiment. As shown in [Supplementary Figure 1](#), the magnetic properties of MFMNPs were introduced into glioblastoma cells and lasted at least 18 days after mouse implantation. Therefore it was predicted that glioblastoma cells into which MFMNPs were introduced immediately after tumor cell transplantation were sufficiently affected by an external magnetic field. Unlike the heterotopic xenograft experiments, the orthotopic experiments were subject to the brain's space limitations, so even in the early stages of tumor growth, it was understood that mice could die depending on the location and direction of the tumor growth.

Conclusion

MNPs have a very high utility value as a contrast agent and a carrier. To use these particles more effectively, they are often used with an external magnetic field. This study dealt with the biological changes induced by MNPs, especially MFMNPs and the external magnetic field, on glioblastoma. The findings suggest that long-term use of MNPs and an external magnetic field is highly involved in the Wnt/ β -catenin signaling pathway and may increase the expression of two mRNAs closely related to tumor growth and metastasis. Both orthotopic and heterotopic xenograft mouse models showed a tendency to accelerate tumor growth. In the heterotopic xenograft model, metastasis to the liver and lungs could be identified, and a trend of increasing mRNA expression was also observed in tumors that had metastasized to the liver. This study did not investigate all the mechanisms of the Wnt/ β -catenin signaling pathway in depth; however, it demonstrated that with MNPs, prolonged exposure to an external magnetic field can cause genetic changes in glioblastoma and changes in tumor growth. This helps understanding of the correlation between MNPs and an external magnetic field.

Future perspective

This study provides guidance on genetic changes in studies that use MNPs and an external magnetic field. Because numerous metal-based nanoparticles are used in nanomedicine (e.g., iron, zinc and manganese), it will be important to extend this type of research to other MNPs and other tumor cells.

Executive summary

- Magnetic nanoparticles have been studied in many applications that use external magnetic fields, but little is known about the genetic changes they cause.
- Manganese ferrite magnetic nanoparticles (MFMNPs) are known not only to have high magnetization but also to obtain ultrasensitive targeted T2 magnetic resonance images *in vivo*.
- Long-term exposure of glioblastoma cells to MFMNPs and an external magnetic field has shown changes in mRNA expression.
- There was no significant change in mRNA expression when MFMNPs or an external magnetic field were used alone.
- When both conditions were satisfied, *LRP6* and *TCF7* mRNA levels were elevated in U-87MG glioblastoma cells.
- *LRP6* and *TCF7* are related to the Wnt/ β -catenin signaling pathway and promote tumor growth and metastasis.
- MFMNPs and an external magnetic field accelerated tumor growth by about 7 days in a heterotopic xenograft animal model.
- MFMNPs and an external magnetic field reduced survival rates, with faster tumor growth, in orthotopic xenograft animal models.
- In a heterotopic xenograft animal model, metastases to the liver and lungs could be confirmed. When affected by MFMNPs and external magnetic field, *TCF7* expression was elevated in metastatic cancer.

Supplementary data

To view the supplementary data that accompany this paper please visit the journal website at: www.futuremedicine.com/doi/suppl/10.2217/nnm-2020-0399

Author contributions

S Yang conceived of this work, carried out experiments and wrote the manuscript. B Kang fabricated and analyzed the manganese ferrite nanoparticles. Y Choi provided technical support during all animal experiments. H Rho gave technical support during qPCR. H Son and Y Huh supervised the entire project, were involved in the designing of all experiments and revised the manuscript. All authors read and approved the final manuscript.

Financial & competing interests disclosure

This research was supported by Development of Measurement Standards and Technology for Biomaterials and Medical Convergence funded by the Korea Research Institute of Standards and Science (KRISS-2020-GP2020-0004) and National Research Foundation of Korea (NRF-2017M3A9G5083322, NRF-2018M3A9E2022828). The authors have no other relevant affiliations or financial involvement with any organization or entity with a financial interest in or financial conflict with the subject matter or materials discussed in the manuscript apart from those disclosed.

No writing assistance was utilized in the production of this manuscript.

Ethical conduct of research

The authors state that they have obtained appropriate institutional review board approval or have followed the principles outlined in the Declaration of Helsinki for animal experimental investigations. All experimental procedures were carried out in accordance with the guidelines of the Institutional Animal Care and Use Committees which were approved by Yonsei University College of Medicine Institutional Animal Care and Use Committee.

Open Access

This work is licensed under the Attribution-NonCommercial-NoDerivatives 4.0 Unported License. To view a copy of this license, visit <http://creativecommons.org/licenses/by-nc-nd/4.0/>

References

Papers of special note have been highlighted as: • of interest; •• of considerable interest

1. Yun S, Shin T-H, Lee J-H *et al.* Design of magnetically labeled cells (mag-cells) for *in vivo* control of stem cell migration and differentiation. *Nano Lett.* 18(2), 838–845 (2018).
2. Shi W, Wang S, Maarouf A *et al.* Magnetic particles assisted capture and release of rare circulating tumor cells using wavy-herringbone structured microfluidic devices. *Lab. Chip* 17(19), 3291–3299 (2017).
3. Lee J-H, Kim ES, Cho MH *et al.* Artificial control of cell signaling and growth by magnetic nanoparticles. *Angew. Chem. Int. Ed. Engl.* 49(33), 5698–5702 (2010).

4. Yang S-H, Heo D, Park J *et al.* Role of surface charge in cytotoxicity of charged manganese ferrite nanoparticles towards macrophages. *Nanotechnology* 23(50), 505702 (2012).
5. Feng Q, Liu Y, Huang J, Chen K, Huang J, Xiao K. Uptake, distribution, clearance, and toxicity of iron oxide nanoparticles with different sizes and coatings. *Sci. Rep.* 8(1), 2082 (2018).
6. Short WO, Goodwill L, Taylor CW, Job C, Arthur ME, Cress AE. Alteration of human tumor cell adhesion by high-strength static magnetic fields. *Invest. Radiol.* 27(10), 836–840 (1992).
7. Raylman RR, Clavo AC, Wahl RL. Exposure to strong static magnetic field slows the growth of human cancer cells *in vitro*. *Bioelectromagnetics* 17(5), 358–363 (1996).
8. Zablotskii V, Dejneka A, Kubinová Š *et al.* Life on magnets: stem cell networking on micro-magnet arrays. *PLoS ONE* 8(8), e70416 (2013).
9. Bae J-E, Huh M-I, Ryu B-K *et al.* The effect of static magnetic fields on the aggregation and cytotoxicity of magnetic nanoparticles. *Biomaterials* 32(35), 9401–9414 (2011).
10. Jia HL, Wang C, Li Y *et al.* Combined effects of 50 Hz magnetic field and magnetic nanoparticles on the proliferation and apoptosis of PC12 cells. *Biomed. Environ. Sci.* 27(2), 97–105 (2014).
- **Helps to understand the combined effects of magnetic field and magnetic nanoparticles.**
11. Rotherham M, El Haj AJ. Remote activation of the Wnt/ β -catenin signalling pathway using functionalised magnetic particles. *PLoS ONE* 10(3), e0121761 (2015).
12. Bae KH, Park M, Do MJ *et al.* Chitosan oligosaccharide-stabilized ferrimagnetic iron oxide nanocubes for magnetically modulated cancer hyperthermia. *ACS Nano* 6(6), 5266–5273 (2012).
13. Subramanian M, Miaskowski A, Jenkins SI, Lim J, Dobson J. Remote manipulation of magnetic nanoparticles using magnetic field gradient to promote cancer cell death. *Appl. Phys. A* 125(4), 226 (2019).
14. Zhang E, Kircher MF, Koch M, Eliasson L, Goldberg SN, Renström E. Dynamic magnetic fields remote-control apoptosis via nanoparticle rotation. *ACS Nano* 8(4), 3192–3201 (2014).
15. Hapuarachchige S, Kato Y, Ngen EJ, Smith B, Delannoy M, Artemov D. Non-temperature induced effects of magnetized iron oxide nanoparticles in alternating magnetic field in cancer cells. *PLoS ONE* 11(5), e0156294 (2016).
16. Klyachko NL, Sokolsky-Papkov M, Pothayee N *et al.* Changing the enzyme reaction rate in magnetic nanosuspensions by a non-heating magnetic field. *Angew. Chem. Int. Ed.* 51(48), 12016–12019 (2012).
17. Lee J-H, Huh Y-M, Jun Y-W *et al.* Artificially engineered magnetic nanoparticles for ultra-sensitive molecular imaging. *Nat. Med.* 13(1), 95 (2006).
- **The first research article to prove that manganese ferrite nanoparticles are more sensitive than other iron oxide-based magnetic nanoparticles in magnetic resonance molecular imaging.**
18. Kim E, Lee K, Huh Y-M, Haam S. Magnetic nanocomplexes and the physiological challenges associated with their use for cancer imaging and therapy. *J. Mater. Chem. B* 1(6), 729–739 (2013).
19. Cho E-J, Yang J, Mohamedali KA *et al.* Sensitive angiogenesis imaging of orthotopic bladder tumors in mice using a selective magnetic resonance imaging contrast agent containing VEGF121/rGel. *Invest. Radiol.* 46(7), 441–449 (2011).
20. Kim E, Lee H, An Y *et al.* Imidazolized magnetic nanovectors with endosome disrupting moieties for the intracellular delivery and imaging of siRNA. *J. Mater. Chem. B* 2(48), 8566–8575 (2014).
21. Yang S-H, Heo D, Lee E *et al.* Galactosylated manganese ferrite nanoparticles for targeted MR imaging of asialoglycoprotein receptor. *Nanotechnology* 24(47), 475103 (2013).
22. Sun S, Zeng H, Robinson DB *et al.* Monodisperse MFe_2O_4 ($M = Fe, Co, Mn$) nanoparticles. *J. Am. Chem. Soc.* 126(1), 273–279 (2004).
23. Yang J, Lee C-H, Ko H-J *et al.* Multifunctional magneto-polymeric nanohybrids for targeted detection and synergistic therapeutic effects on breast cancer. *Angew. Chem. Int. Ed. Engl.* 46(46), 8836–8839 (2007).
24. Ji Y, Oh S, Kang SG *et al.* Terahertz reflectometry imaging for low and high grade gliomas. *Sci Rep.* 6, 36040 (2016).
25. Lee E, Yang J, Ku M *et al.* Metabolic stress induces a Wnt-dependent cancer stem cell-like state transition. *Cell Death Dis.* 6(7), e1805 (2015).
- **Helps to select Wnt signaling-related mRNA.**
26. Houpt TA, Pittman DW, Barranco JM, Brooks EH, Smith JC. Behavioral effects of high-strength static magnetic fields on rats. *J. Neurosci.* 23(4), 1498 (2003).
27. Chakeres DW, Kangarlou A, Boudoulas H, Young DC. Effect of static magnetic field exposure of up to 8 Tesla on sequential human vital sign measurements. *J. Magn. Reson. Imag.* 18(3), 346–352 (2003).
28. Brennan K, Gonzalez-Sancho JM, Castelo-Soccio LA, Howe LR, Brown AMC. Truncated mutants of the putative Wnt receptor LRP6/Arrow can stabilize β -catenin independently of Frizzled proteins. *Oncogene* 23(28), 4873–4884 (2004).
29. Björklund P, Svedlund J, Olsson A-K, Çkerström G, Westin G. The internally truncated LRP5 receptor presents a therapeutic target in breast cancer. *PLoS ONE* 4(1), e4243 (2009).

30. Li Y, Lu W, He X, Schwartz AL, Bu G. LRP6 expression promotes cancer cell proliferation and tumorigenesis by altering β -catenin subcellular distribution. *Oncogene* 23(56), 9129–9135 (2004).
31. Yao Q, An Y, Hou W *et al.* LRP6 promotes invasion and metastasis of colorectal cancer through cytoskeleton dynamics. *Oncotarget* 8(65), 109632–109645 (2017).
- **Helps understand the role of LRP6.**
32. Zarkou V, Galaras A, Giakountis A, Hatzis P. Crosstalk mechanisms between the WNT signaling pathway and long non-coding RNAs. *Noncoding RNA Res.* 3(2), 42–53 (2018).
33. Benhaj K, Akcali KC, Ozturk M. Redundant expression of canonical Wnt ligands in human breast cancer cell lines. *Oncol. Rep.* 15(3), 701–707 (2006).
34. Jin FS, Wang HM, Song XY. Long non-coding RNA TCF7 predicts the progression and facilitates the growth and metastasis of colorectal cancer. *Mol. Med. Rep.* 17(5), 6902–6908 (2018).
35. Mayer K, Hieronymus T, Castrop J, Clevers H, Ballhausen WG. Ectopic activation of lymphoid high mobility group-box transcription factor TCF-1 and overexpression in colorectal cancer cells. *Int. J. Cancer* 72(4), 625–630 (1997).
36. Mandawala C, Chebbi I, Durand-Dubief M *et al.* Biocompatible and stable magnetosome minerals coated with poly-L-lysine, citric acid, oleic acid, and carboxy-methyl-dextran for application in the magnetic hyperthermia treatment of tumors. *J. Mater. Chem. B* 5(36), 7644–7660 (2017).
37. Cai Q, Fan Q, Buechlein A *et al.* Changes in mRNA/protein expression and signaling pathways in *in vivo* passaged mouse ovarian cancer cells. *PLoS ONE* 13(6), e0197404 (2018).
38. Hernandez A, Smith F, Wang Q, Wang X, Evers BM. Assessment of differential gene expression patterns in human colon cancers. *Ann. Surg.* 232(4), 576 (2000).
39. Chen W-Y, Liu S-Y, Chang Y-S *et al.* MicroRNA-34a regulates WNT/TCF7 signaling and inhibits bone metastasis in Ras-activated prostate cancer. *Oncotarget* 6(1), 441 (2014).
40. Xu X, Liu Z, Tian F, Xu J, Chen Y. Clinical significance of transcription factor 7 (TCF7) as a prognostic factor in gastric cancer. *Med. Sci. Monit.* 25, 3957–3963 (2019).
- **Helps understand the role of TCF7.**